



A. Zalizovski^{1, 2, 3 *}, Y. Yampolski², I. Stanislawska³, O. Koloskov^{1, 2, 4},
O. Budanov², O. Bogomaz⁵, B. Gavrylyuk^{1, 2}, A. Sopin^{1, 2},
A. Reznychenko^{2, 3}, A. Kashcheyev⁴, S. Kashcheyev², V. Lisachenko²

¹ State Institution National Antarctic Scientific Center, Ministry of Education and Science of Ukraine, Kyiv, 01601, Ukraine

² Institute of Radio Astronomy, National Academy of Sciences of Ukraine, Kharkiv, 61002, Ukraine

³ Space Research Centre of Polish Academy of Sciences, Warsaw, 00-716, Poland

⁴ Department of Physics, University of New Brunswick, Fredericton, NB E3B5A3, Canada

⁵ Institute of Ionosphere, National Academy of Sciences of Ukraine and Ministry of Education and Science of Ukraine, Kharkiv, 61001, Ukraine

*Corresponding author: zaliz@rian.kharkov.ua

Long-distance HF radio waves propagation during the April 2023 geomagnetic storm by measurements in Antarctica, in Europe, and aboard RV *Noosfera*

Abstract. The paper aims at an experimental study of the mechanisms of long-distance high-frequency (HF) propagation and spatial and temporal variations of the ionospheric parameters during the first hours of a severe geomagnetic storm of April 23, 2023 by spatially separated measuring equipment located at the research vessel (RV) *Noosfera*, the Ukrainian Antarctic Akademik Vernadsky station (hereinafter *Vernadsky*), and the LOFAR observatory PL610 in Borowiec (Poland). High-frequency vertical and oblique sounding techniques of the ionosphere were used. Geospace measurements were carried out synchronously. During the first hours of the geomagnetic storm of April 23–24, 2023, unexpectedly well-correlated variations in the Doppler frequency shifts of HF signals emitted from *Vernadsky* were observed at the RV *Noosfera* and the PL610 station. Furthermore, variations in Doppler frequency shifts of HF signals strongly correlate with magnetic field records in Antarctica and Poland. Variations in the frequency of HF signal spectral components, distinguishable during storm conditions, are utilized to clarify the mechanism of long-distance HF propagation and estimate the vertical velocity of ionospheric layers. Signals of HF CHU time radio station (Canada) at 7850 and 14670 kHz were unexpectedly observed in all receiving sites. Most probably, the CHU station radio signals registered during the initial stage of the geomagnetic storm were scattered on the polar ovals' ionospheric inhomogeneities and propagated further along the return (long arc of the great circle) paths. Redistribution of the ionospheric plasma during the geomagnetic storm leads to the formation of HF radio propagation channels absent under quiet conditions.

Keywords: Doppler HF receiver, ionosonde, geomagnetic field, ionosphere

1 Introduction

The long-distance propagation of high frequency (HF) radio waves (further than 10000 km) was the only way that provided the human civilization with reliable wireless communication worldwide before the space age. Scientific and technical interest in this subject, driven by practical applications, persisted until the 1970s and 1980s. However, the outcomes of those studies were likely constrained by the limited availability of open-source literature, as there were few articles freely accessible at that time (for instance, Stein, 1958; Muldrew & Maliphant, 1962; Shlionsky, 1979; Gurevich & Tsedilina, 2011). With the development of satellite communication technology (Ludwig, 2011), the practical significance of ionospheric HF propagation diminished. At the same time, with the development of the computer era, previously unavailable possibilities of digital signal processing emerged around the 1990s, making it possible to study features of long-distance propagation mechanisms in the frequency-time domain. By employing the time-frequency analysis of HF signals propagating over long-distance radio paths, one can address inverse problems of restoring the characteristics of ionospheric inhomogeneities of various scales that influence such propagation.

Ionospheric propagation of HF radio waves is one of the primary scientific areas at the Institute of Radio Astronomy of the National Academy of Sciences of Ukraine. At the very beginning of the 2000s, the first Doppler receivers of the Institute were delivered to the Ukrainian Antarctic Akademik Vernadsky station (65.25 °S, 64.25 °W) (hereinafter *Vernadsky*). It was then that the first results measurements of propagation of HF radio signals with a receiving site on board the research vessel, as well as radio oceanographic data from ionospheric signals, were obtained (Kashcheev et al., 2001; Kashcheyev et al., 2003). First Doppler HF receivers were installed on *Vernadsky* in 2002. During that expedition, the first results were obtained using the signals of time signal stations in the Northern Hemisphere propagating toward

the Antarctic Peninsula (Zalizovskii et al., 2007). At the same time, the measurements of HF signals transmitted by powerful ionospheric heaters on long radio paths were started (Litvinenko & Yampolsky, 2005; Galushko et al., 2008; Zalizovski et al., 2009), as well as the study of nonlinear mechanisms of excitation of ionospheric channels of long-distance HF radio wave propagation (Yampolski et al., 2019).

Routine measurements of HF radio signals of the North American CHU (47.29° N, 75.76° W) and European RWM (56.74° N, 37.62° E) time signal radio stations on long radio paths were started in 2010 at *Vernadsky* (Zalizovski et al., 2015). Since that time, the global network of digital Doppler receivers of the Institute of Radio Astronomy has been significantly extended (Koloskov et al., 2014). Unfortunately, part of that network operating on the territory of Ukraine has been lost since the beginning of Russia's full-scale invasion. However, a dual-channel Doppler HF receiver as well as a passive oblique ionosonde receiving signals from an active one that was operating at the observatory of the Institute of Ionosphere of the National Academy of Sciences and Ministry of Education and Science of Ukraine near Zmiiv, Ukraine (49.68° N, 36.29° E) were deployed at the LOFAR observatory PL610 in Borowiec, Poland (52.27° N, 17.07° E) (further in the text – PL610).

A significant step in experimental studies of the ionosphere at *Vernadsky* was the introduction of a portable Doppler ionosonde (Zalizovski et al., 2018; 2020; Koloskov et al., 2023). Since 2022, a new ionosonde receiving position equipped with two stationary crossed antennas has been added, which made it possible to automatically separate the magneto-ionic components in the ionograms (Koloskov et al., 2023).

A significant milestone in the development of geospace research of the long-distance propagation of HF radio signals was the installation of a radiophysical observatory on board the research vessel (RV) *Noosfera*. This observatory was employed during the vessel's voyages to Antarctica in 2022 (Zalizovski et al., 2022) and 2023. During

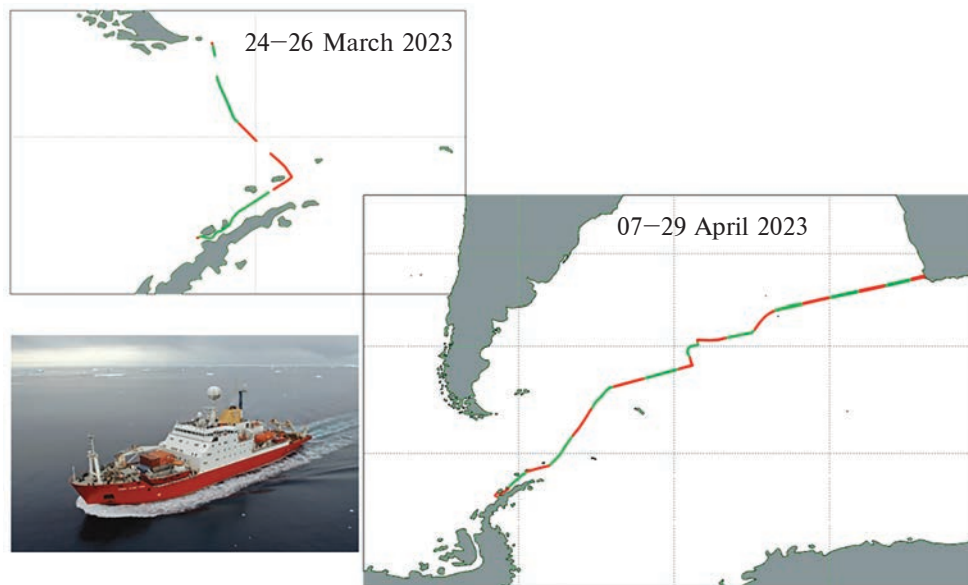


Figure 1. The RV *Noosfera*'s route during the measuring campaign in March–April 2023. Each red and green part of routes shows the duration of one day

her first trip to Antarctica in January–April 2022, a dual-channel Doppler HF receiver, a passive oblique ionosonde, and very low-frequency equipment were installed onboard. The same equipment, but without the very low-frequency part, was deployed and used in the March–April 2023 measuring campaign. This paper presents the inaugural description of the radiophysical observatory on the RV *Noosfera*.

This work aims to suggest mechanisms of long-distance HF propagation during the commencement and first hours of a powerful geomagnetic storm on April 23, 2023, as well as to study spatial and temporal variations of the ionospheric conditions at the beginning of this storm using spatially separated measuring equipment located at the RV *Noosfera*, *Vernadsky*, and the PL610 observatory of the LOFAR network.

2 Methods and data

2.1 General characteristics of the measuring campaign of March–April 2023

As mentioned above, we will focus on the results of a comprehensive multi-position measuring cam-

paigned to study the ionospheric dynamics and long-distance HF propagation using ground-based observational sites and sea measuring positions on board the RV *Noosfera*. The RV *Noosfera*'s route during the measuring campaign is shown in Figure 1.

During the March–April 2023 measurements, the RV *Noosfera* was provided with the following equipment: a dual-channel Doppler HF receiver, based on WiNRADiO devices (Koloskov et al., 2014 and references therein); passive oblique ionosonde, capable of receiving signals transmitted by the active ionosonde operating at *Vernadsky* (Zalizovski et al., 2018; Koloskov et al., 2023); Garmin 18 GPS signal receiver serving the dual purpose of providing continuous data regarding the location, speed and direction of the RV *Noosfera* movement (see Fig. 1), and ensuring time synchronization of the ionosonde and the HF receiver; two HF antenna-feeder systems: the vertical dipole, which was connected to the dual-channel receiver, and the tilted dipole, from which the signal was fed to the passive ionosonde, deployed on the direction-finding deck of the ship (Fig. 2).

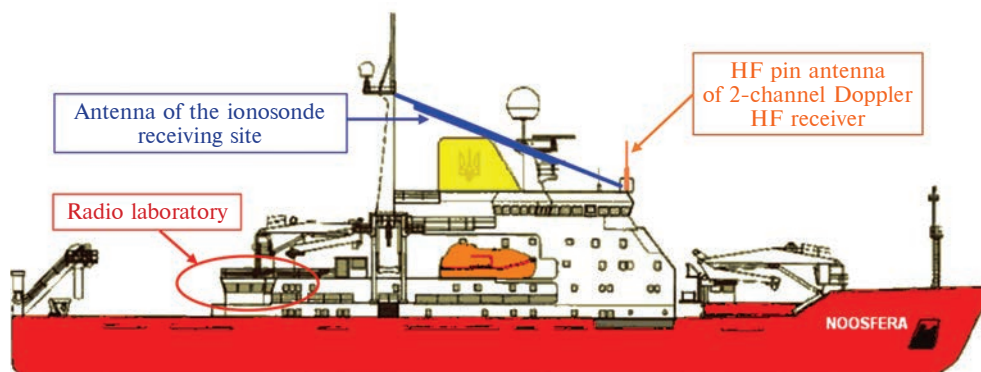


Figure 2. The location of HF antennas on board the RV *Noosfera* during the March–April 2023 measuring campaign

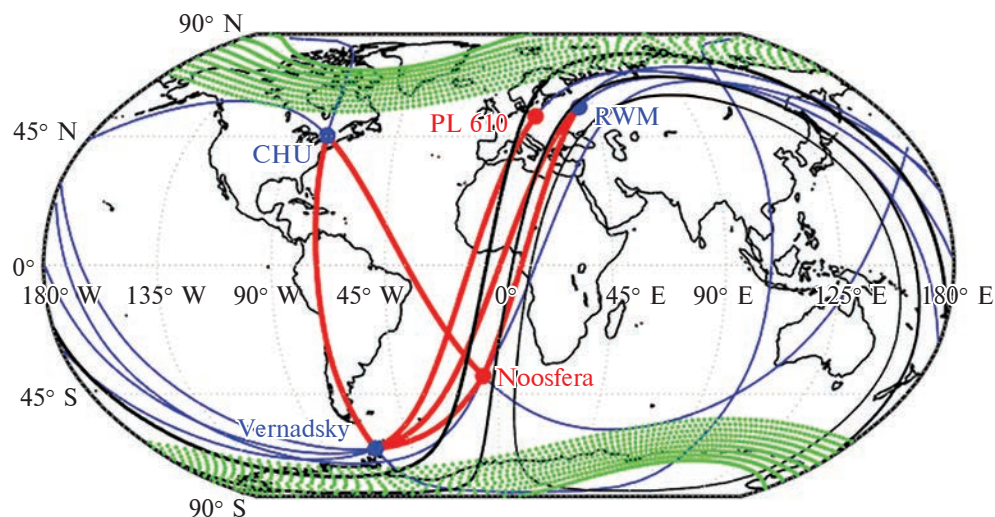


Figure 3. Experiment layout for April 23, 2023 at 18:00 UT. Red lines show direct radio paths, blue lines – return paths, sun terminator marked by black lines (thick – on the surface, thin – at heights of 100 and 300 km; it was daytime in America continents and nighttime in Asia and Australia). Green lines show the most probable location of the equatorial boundary of auroral ovals for planetary Kp ~0...6

Connection cables were laid from the antennas to the radiophysics laboratory on the second deck of the ship (Fig. 2). The length of each cable was approximately 75 meters.

Two active ionosondes were operated at *Vernadsky*: the traditional IPS-42, and a software-defined radio (SDR-based) ionosonde (Koloskov et al., 2023), which was upgraded in 2022. The deployment of a new stationary antenna system allows to distinguish the magnetoionic components

of radio signals reflected from the ionosphere (Koloskov et al., 2023). Furthermore, a low-power (less than 100 W) monochromatic signal was emitted from *Vernadsky* at the carrier frequencies determined on board the RV *Noosfera*, guided by the analysis of oblique ionograms. Besides the ionosondes, the measuring system at *Vernadsky* includes the Argentine Island Archipelago (AIA) geomagnetic observatory and a dual-channel Doppler HF receiver similar to the one operating on

board the RV *Noosfera*. The same receiver (Koloskov et al., 2014) was used at PL610.

2.2 Experiment design

To analyze the features of HF propagation, the spectrograms of radio signals emitted from *Vernadsky* (65.25° S, 64.27° W) and HF time signal radio stations located in the Northern Hemisphere: the CHU station (45.30° N, 75.75° W) and the RWM station (55.72° N, 38.20° E), and were received at *Vernadsky*, RV *Noosfera* (38.69° S, 06.56° W at 18:00 UT on April 23, 2023, coordinates continuously changed over time), and at the PL610 LOFAR station (52.28° N, 17.08° E) were calculated. The map of the transmitting and receiving sites, direct and return radio paths, as well as the probable locations of the auroral ovals for low and moderate geomagnetic disturbances, are shown in Figure 3.

The first channel of the Doppler receivers at RV *Noosfera*, *Vernadsky*, and the PL610 station recorded the signals of the RWM station at frequencies of 4996, 9996, and 14996 kHz, and the CHU station at frequencies of 3330, 7850, and 14670 kHz. The receivers were tuned automatically in a half-hourly cycle, as shown in Table 1.

Table 1. A 30-minute cycle of registration of CHU and RWM time stations signals by Doppler receivers operating at the RV *Noosfera*, *Vernadsky*, and the PL610 station

Frequency change time, *:MM:SS	Carrier frequency, Hz
*:00:00	4996000
*:02:30	9996000
*:05:00	14996000
*:09:00	7850000
*:15:00	3330000
*:17:30	14670000
*:19:50	4996000
*:23:20	9996000
*:26:40	14996000

The analysis of these signals at the specific frequency consisted of calculating average power spectra with a time resolution equal to the period of the changing frequency cycle (except the period from 20 to 30 minutes when the RWM station operates in pulse mode with 10 Hz repetition frequency). Daily spectrograms of CHU and RWM stations' signals for each receiving site are represented by a set of 48 average power spectra constructed every half-hour.

During the April 23, 2023 event a monochromatic continuous signal at a frequency of 25277 kHz with a power of slightly less than 100 W was emitted from *Vernadsky*. The second channels of the receivers at the RV *Noosfera* and the PL610 station recorded that signal. The second channel of the receiver at *Vernadsky* was constantly tuned to the frequency of 9996 kHz emitted by the RWM station. The morphological features of the signal spectrograms were compared with the variations of the components of the geomagnetic field recorded at the AIA observatory, the BEL observatory (Belsk Duży, Poland, 51.83° N, 20.789° E), and the ASC observatory (Ascension Island, 7.949° S, 14.376° W). In addition, the ionograms of the vertical sounding of the ionosphere from *Vernadsky* and the ionograms of the oblique sounding obtained on board the RV *Noosfera* were analyzed.

2.3 Doppler HF sounding of the ionosphere

During the commencement of the geomagnetic storm, rapid variations in the Doppler frequency shift were observed since 17:36 UT in the spectrograms of signals emitted from *Vernadsky* and recorded on board the RV and at PL610. As can be seen from the spectrograms (Figs. 4, 5), a sudden start of variations is observed at both points at approximately 17:36 UT, after which almost synchronous variations of the Doppler frequency shifts are observed at PL610 (the approximate distance from the transmitter at *Vernadsky* is 14770 km) and at the RV for about two more hours (the distance to *Vernadsky* at the time of the start of the storm is about 4700 km).

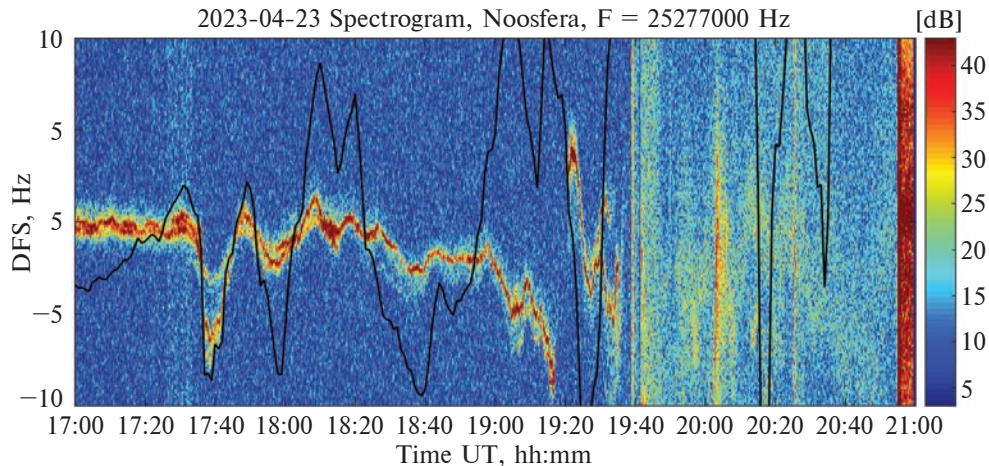


Figure 4. Spectrograms of the signal emitted from *Vernadsky* at 25277 kHz, received at RV *Noosfera*, with the X component of the geomagnetic field measured at AIA (black line)

Comparison of the spectrograms with variations of the components of the geomagnetic field allows us to conclude that the highest correlation of the variations of the magnetic field in the first two hours of the geomagnetic storm is observed with the X component at the AIA observatory and the anti-correlation with the Y component at the BEL observatory (Figs. 4, 5 show those components of magnetic field superposed with spectrograms). In addition, during the negative variation of the Doppler frequency shift at 17:36–17:46 UT, it can be seen several spectral components in the spectrograms, whose variations are proportional to each other in the first approximation. Possible reasons for this will be discussed below.

We will further analyze the features of variations in the parameters of the HF signals of the time signal radio stations, which were received at different sites. Signals were recorded with the same frequency-changing cycle shown in Table 1. Daily spectrograms were calculated according to the algorithm described above. The mentioned approach does not allow us to analyze the rapid dynamics of variations of the signals. However, it allows measuring the features and differences of the signal propagation characteristics on the storm day compared to quiet days.

Consequently, through the analysis of the spectrograms presented in Figure 6, it is possible to compare the signal behavior of the RWM station on the specific disturbed day of April 23, 2023, with the 26-day average under normal conditions (spanning April 1 – 27, 2023, excluding April 23). It can be noted that no peculiarities were observed on April 23 at the frequency of 4996 kHz (Fig. 6 a, d). At the frequency of 9996 kHz on April 23 in the interval of 17–20 UT, a signal with a signal-to-noise ratio of up to 20 dB appears (Fig. 6 b), which is absent in the monthly averaged spectrograms (Fig. 6 e). The signal at the frequency of 14996 kHz shows more significant variations of the Doppler frequency shift during the beginning of the storm (Fig. 6 c) compared to other days of the month (Fig. 6 f).

Similar processing was implemented for CHU signals received at *Vernadsky*. It should be noted that at 3330 kHz, no effects were observed at the beginning of the storm (Fig. 7 a, d). However, at 7850 and 14670 kHz, the effect of the appearance of a rather powerful signal at *Vernadsky* looks very convincing. As can be seen, from 19 to 20 UT, a signal appears on 7850 kHz (Fig. 7 b), which is absent on other days of the month (Fig. 7 e). The situation is similar for the signal at 14670 kHz: at 19–20 UT, a signal appears that is absent on other days (Fig. 7 c, f).

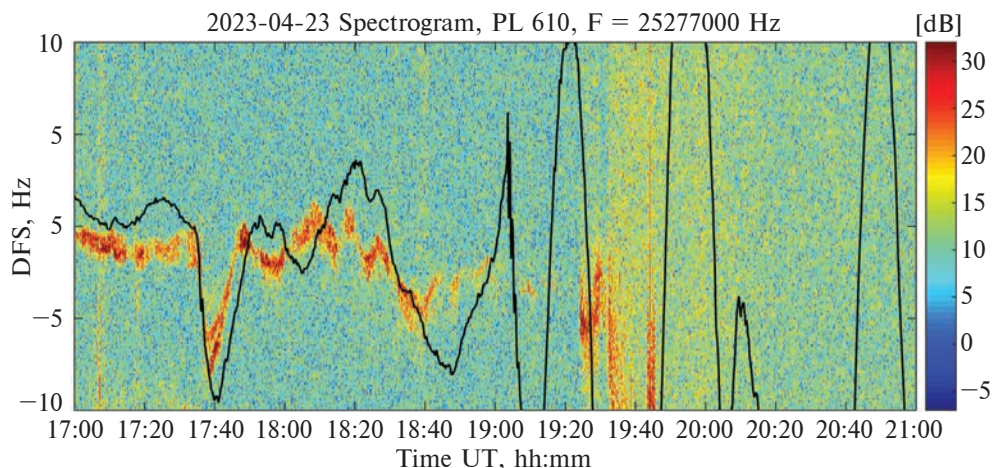


Figure 5. Spectrograms of the signal emitted from *Vernadsky* at 25277 kHz received at PL610, with the “-Y” component of the geomagnetic field measured at BEL (black line)

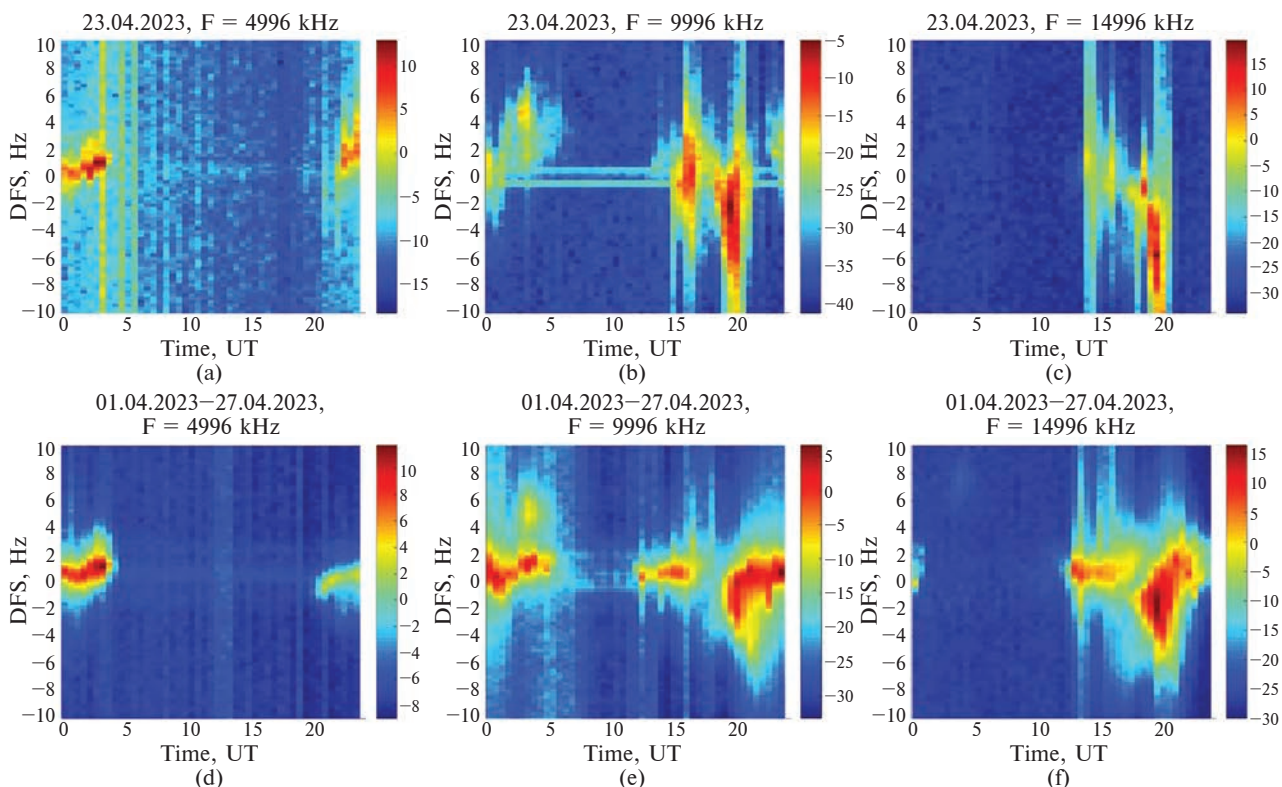


Figure 6. Daily spectrograms of RWM station signals at the frequencies of 4996 (a, d), 9996 (b, e), and 14996 kHz (c, f), received at *Vernadsky* on April 23, 2023 (a–c), and averaged daily spectrograms for April 1–27, 2023, except April 23, 2023 (d–f)

We cannot fully implement the aforementioned processing techniques for the RWM and CHU data recorded onboard RV *Noosfera* due to the movement

of the reception point. Therefore, a reference time interval was limited by five days to compare the spectra with neighboring days (19–20 and 24–26 April, 2023).

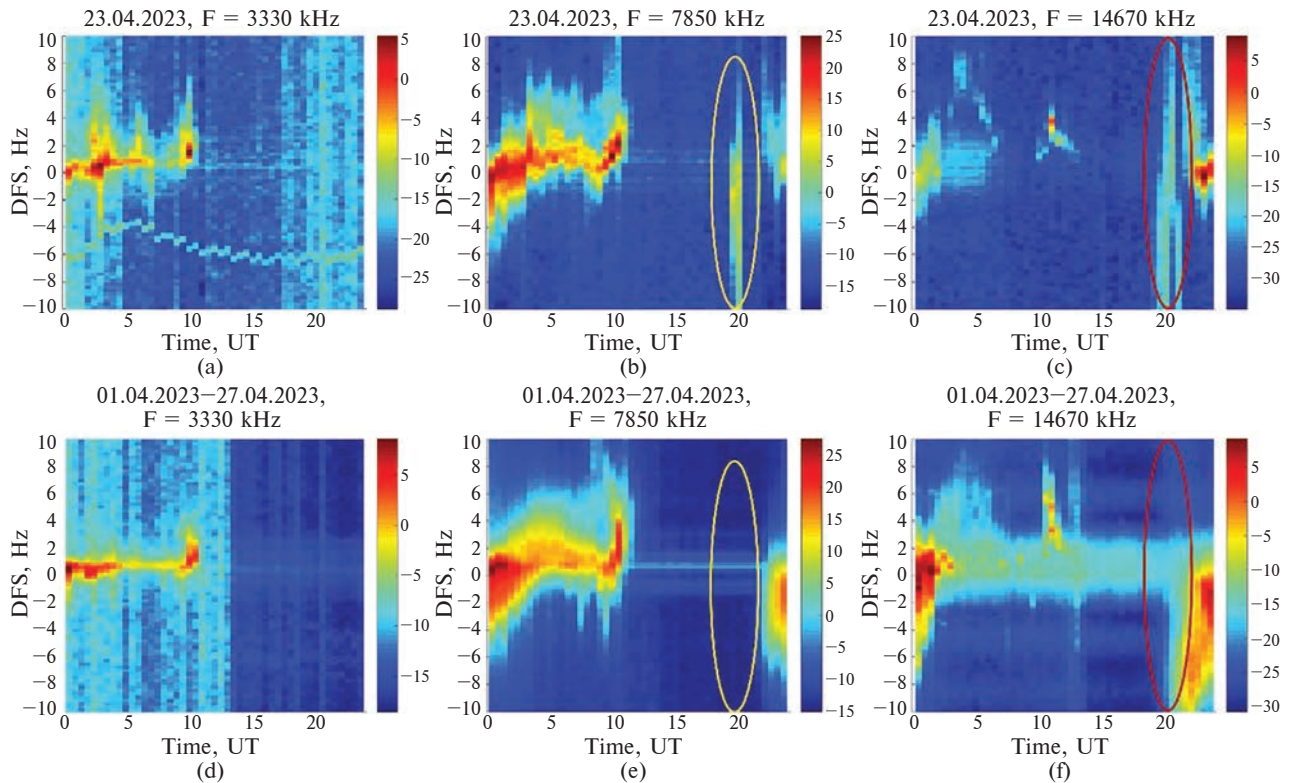


Figure 7. Daily spectrograms of the CHU station signals at the frequencies of 3330 (a, d), 7850 (b, e), and 14670 kHz (c, f), received at *Vernadsky* on April 23, 2023 (a–c), and averaged daily spectrograms for April 1–27, 2023, except April 23, 2023 (d–f). The ellipses on (b, c, e, f) show the time interval of signal appearance (daily spectrograms) or its absence on the averaged ones

Figure 8 compares the RWM station signals recorded on April, 23, 2023 with neighboring days. There is a noticeable increase in the signal level of 4996 kHz at 17:30–20:00 (Fig. 8 a) compared with the background days (Fig. 8 d). At the frequencies of 9996 and 14996 kHz, the first effect is the absence of a signal propagating through the reverse path on April 23, 2023 (Fig. 8 b, c, signal with nearly zero Doppler shift from 12 to 17 UT), compared with the background days (Fig. 8 e, f). During the beginning of the storm from 17 to 20 UT, a rather powerful signal was observed at 9996 and 14996 kHz (Fig. 8 b, c), almost the same as during the reference days (Fig. 8 d, e). The difference on the storm day is the decrease in the intensity of the 9996 kHz signal and the disappearance of the 14996 kHz signal after 20:00 UT. Comparing the signals of the CHU

station, it is possible to note the absence of discrepancies at the frequency of 3330 kHz (Fig. 9 a, d) and the appearance of signals at the frequencies of 7850 (Fig. 9 b) and 14670 kHz (Fig. 9 c) at 19–20 UT (which are absent on other days (Fig. 9 e, f)), very similar to that observed at *Vernadsky* (Fig. 7 b, c).

2.4 Frequency and time analysis of 10 Hz pulse mode of RWM signal received at *Vernadsky* and *Noosfera*

At *Vernadsky* and on board the RV *Noosfera* (during her journey from *Vernadsky* to Cape Town), the time synchronization of the Doppler HF receivers was organized by mixing of GPS pulse per second (PPS) signals once an hour into the RF receiving circuit. This made it possible to measure the length of the propagation path of the signals of the RWM station during its operation in pulse

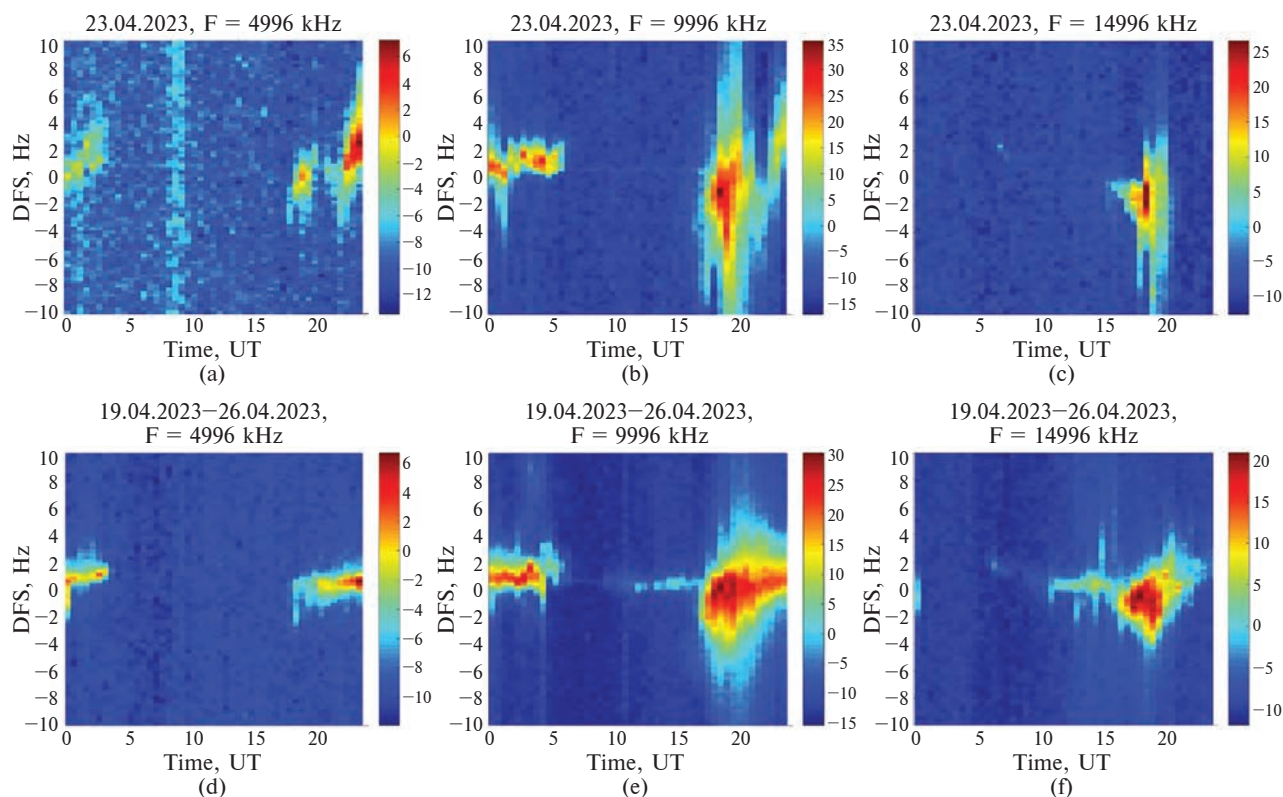


Figure 8. Daily spectrograms of the RWM station signals at the frequencies of 4996 (a, d), 9996 (b, e), and 14996 kHz (c, f), received at RV *Noosfera* on April 23, 2023 (a–c), and averaged daily spectrograms for April 20–21, and 24–26, 2023 (d–f)

mode with a repetition frequency of 10 Hz. The processing used here is described in detail by Kashcheev et al. (2013). It consists of calculating the Fourier transform from signal samples taken with a pulse repetition rate of 10 Hz and duration of 10 s. Thus, we get overlap in the frequency domain due to neglecting the conditions of the Nyquist–Shannon sampling theorem. However, the “Doppler frequency shift – time of delay” diagram obtained by plotting the set of such spectra give us the visualization where the signal modes could be separated by both time and spectral features.

Let us examine the spectral and temporal structure of the signals during the geomagnetic storm. The signal at a frequency of 9996 kHz at 18:54–18:56 UT arrives at the RV *Noosfera* by two modes (Fig. 10 a). The first mode, characterized by the Doppler frequency shift of less than 2.5 Hz, has

a group path length of approximately 12000 km, while the second mode, with the Doppler frequency shift of more than 2.5 Hz, corresponds to a group path length of 13500 km. Since the direct distance along the Earth’s surface between the RWM station and the RV *Noosfera* at 18:55 UT was 11307 km, it is evident that all spatial modes were propagated relatively close to the direct path.

A tilt of the pulse front (Fig. 10, the leading edge of pulses are marked in black) is observed for the second mode (according to the spectrogram for this signal in Fig. 8 b, the sign of the Doppler frequency shift around 19:00 UT was negative). The propagation path length increases with an increase in the module of Doppler frequency shift (Fig. 10 a). This feature could be explained by focusing on the global irregularity moving away from the direct propagation path. The anal-

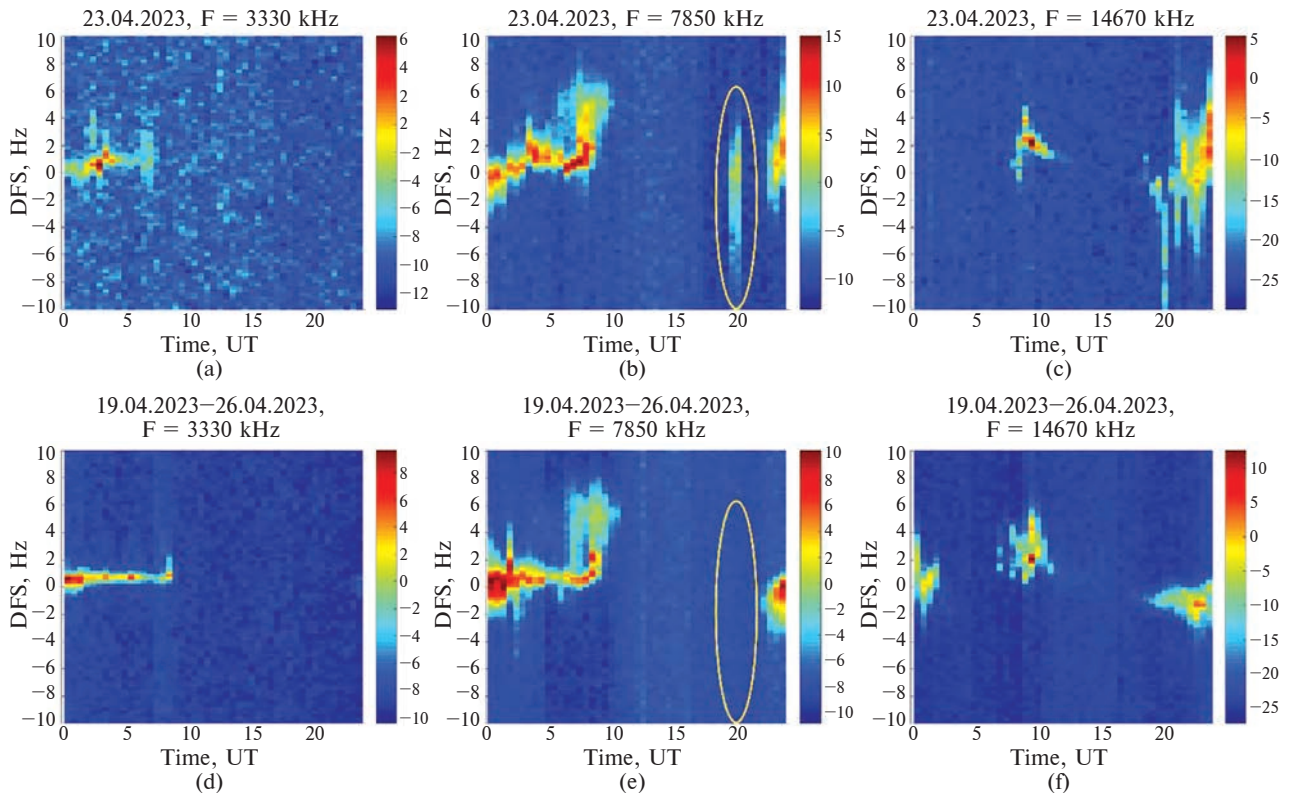


Figure 9. Daily spectrograms of the CHU station signal at the frequencies of 3330 (a, d), 7850 (b, e), and 14670 kHz (c, f), received at RV *Noosfera* on April 23, 2023 (a–c), and averaged daily spectrograms for April 20–21, and 24–26, 2023 (d–f)

ysis of the experiment scheme (Fig. 3) permits us to conclude that, most likely, the solar terminator is the source of that inhomogeneity.

According to the registration at *Vernadsky*, we also see significant signal dispersion (Fig. 10 b). The first components of the signal have a path length of 16300 km, the later components shifted by about 4 Hz of the Doppler frequency shift moduli (taking into account the sign of the signal spectrum in Figure 6 b, the actual Doppler frequency shift is -4 Hz), propagate along paths of about 17000 km. Note that the distance between *Vernadsky* and the RWM station by the Earth’s surface is 15930 km. A sample of pulse selection for the RWM station signals at 14996 kHz is shown in Figure 10 c, d for integration over the time interval 17:57–17:59 UT. The tilt of the pulse front is observed both at *Vernadsky* and at the

RV *Noosfera*, which indicates the propagation of energy along many trajectories rather than one.

2.5 Vertical sounding of the ionosphere

During the geomagnetic storm event of 23 April, 2023, regular vertical sounding of the ionosphere was provided at *Vernadsky* by two active ionosondes, IPS-42, which has been operating at *Vernadsky* since 1983 (Broom, 1984), and the SDR-based ionosonde, which started to operate in 2017. Signals from the digital ionosonde were also used for passive oblique sounding on board the RV *Noosfera*. Upon departure from the Arctowski Station, the operation mode was altered due to a significant increase in the distance between the transmitting and receiving locations. This adjustment involved running exclusively ionograms every 5 minutes (Dop-

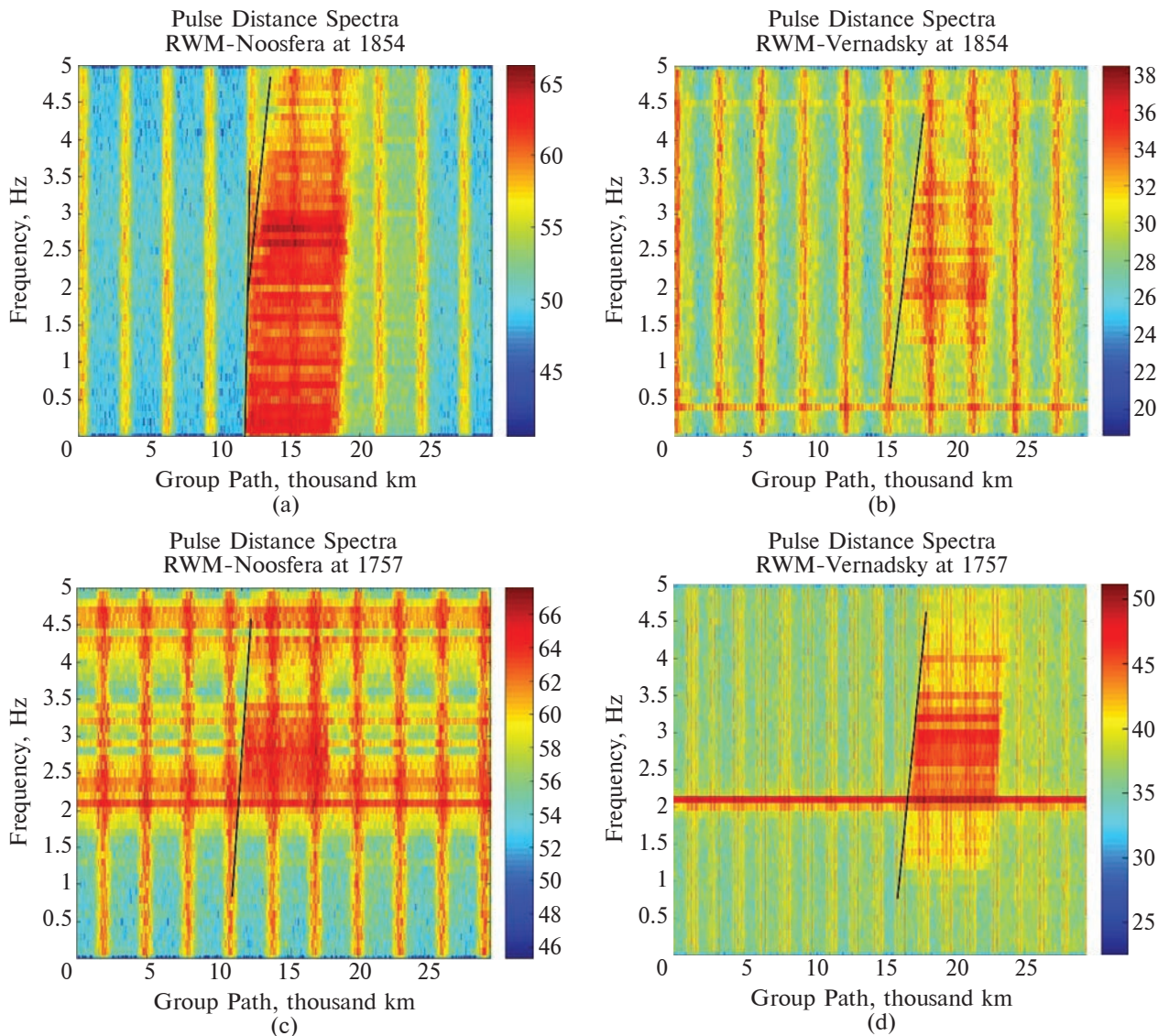


Figure 10. “Doppler frequency shift – Group path” diagrams of the RWM station signals received at RV *Noosfera* (a, c) and *Vernadsky* (b, d) on 23 April 2023 at 18:54–18:56 UT at a frequency of 9996 kHz (a–b), and at 17:57–17:59 UT at a frequency of 14996 (c–d). Black line shows the position of leading edge of pulse

pler soundings were discontinued), and the upper frequency limit for the ionograms was raised to 30 MHz. It should be noted that all ionosondes operate in the local solar time of *Vernadsky* (LT), which is 4 hours less than UT (LT = UT – 4h).

Let us consider the ionospheric-sounding data recorded at *Vernadsky* during the commencement of the storm. The height-time diagram for April

23, 2023, according to the IPS-42 ionosonde, is shown in Figure 11 a, and the averaged (median) height-time diagram (the technique was described by Zalizovski et al., 2020; 2021) for April 2023 is shown on Figure 11 b. From 13:30 to 13:45 LT, the ionosphere lifted by about 15 km (Fig. 11 a). At this time, the spectrograms of the *Vernadsky* signal of 25277 kHz received at the RV *Noosfera* (Fig. 4) and the PL610 station (Fig. 5) simulta-

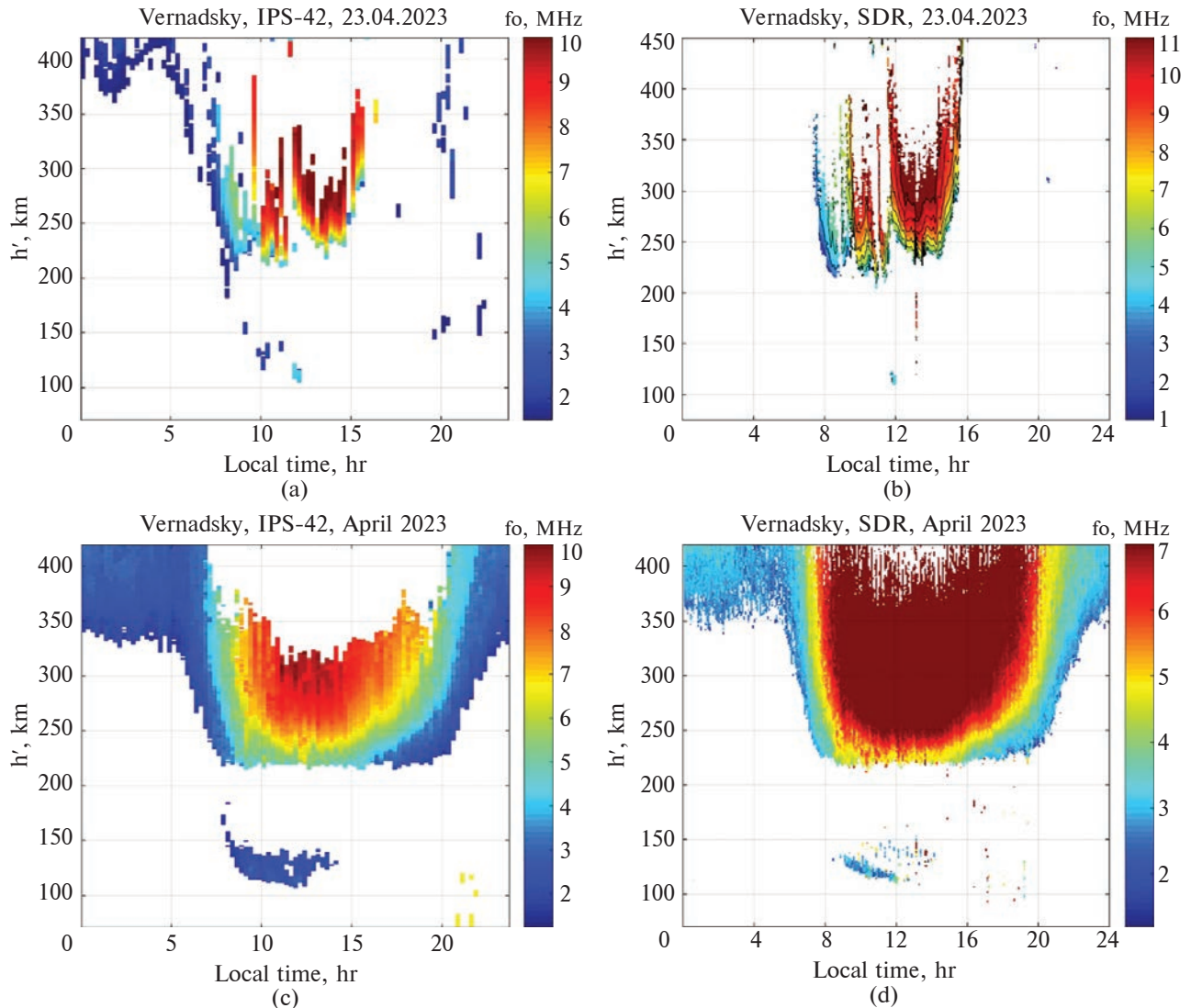


Figure 11. The height-time diagrams of the vertical sounding of the ionosphere at *Vernadsky*: (a, c) for April 23, 2023; (b–d) median diagram for April 2023; (a–b) according to IPS-42 data; (c–d) according to digital ionosonde data

neously show the negative variations in the Doppler frequency shift.

The SDR-based ionosonde performed sounding with a time resolution of 5 minutes. First, at 13:35–13:40 LT, the ionospheric plasma moved upward rather quickly, approximately 15 km in 5–10 minutes (Fig. 11c), which allows us to estimate the maximum vertical velocity to be 25–50 m s⁻¹. According to both ionosondes, plasma moved rapidly upward at 15–16 LT. The reflections from the ionosphere disappeared completely after 16:00 LT (20:00

UT) compared to monthly medians (Fig. 11 c, d). At the same time, the 25277 kHz signal transmitted from *Vernadsky* was no longer detected at the RV *Noosfera* and the PL610 station after 20:00 UT.

2.6 Oblique ionospheric sounding with receiving site on board the RV *Noosfera*

The oblique ionograms were recorded at the RV *Noosfera* using the signals of the SDR-based ionosonde operating at *Vernadsky*. The last ionogram during the geomagnetic storm under consideration

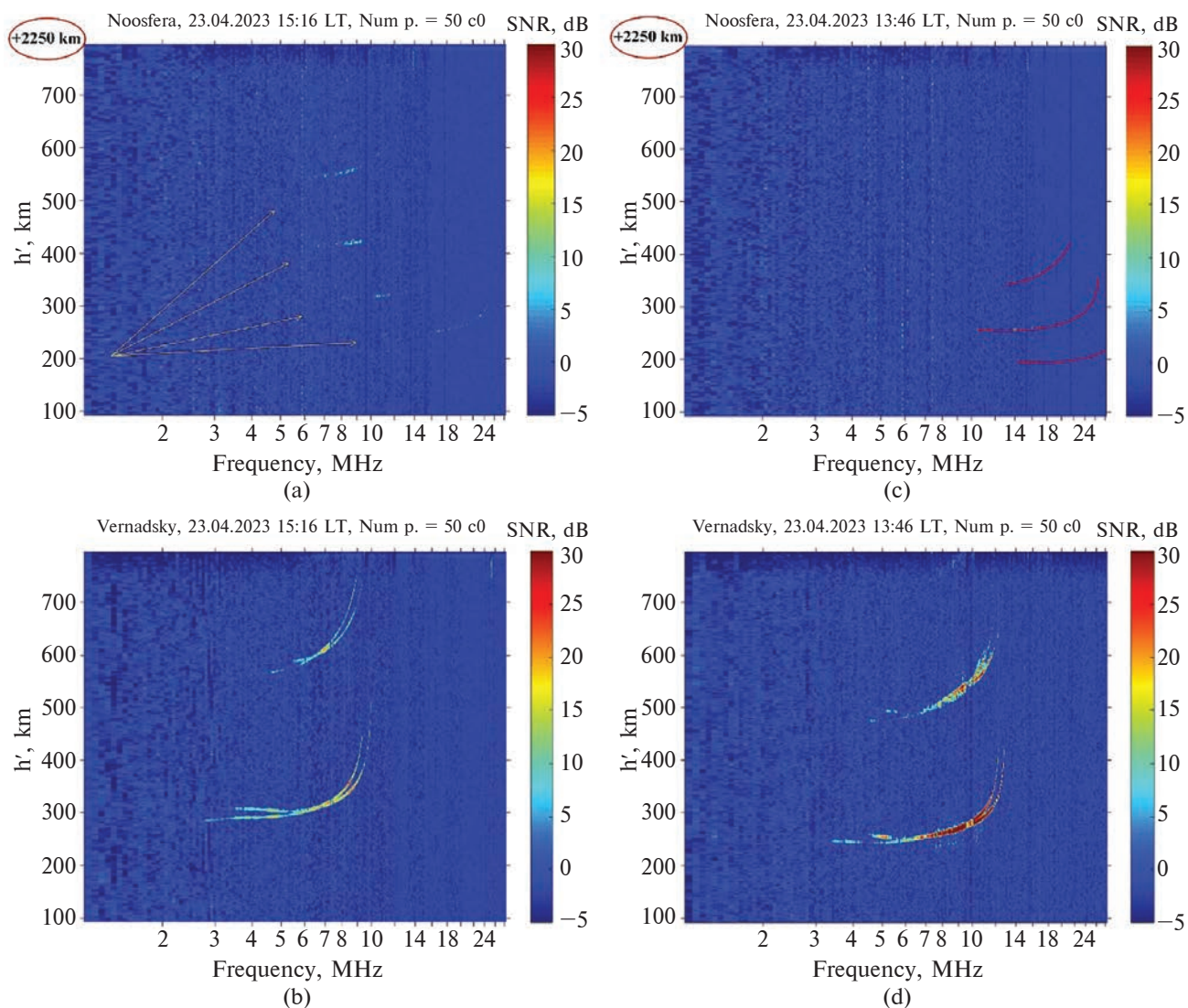


Figure 12. Oblique ionograms registered at the RV *Noosfera* (a, c); corresponding vertical ionograms registered at *Vernadsky* (b, d); on April 23, 2023, at 15:16 LT (19:16 UT) (a–b) and at 13:46 LT (17:46 UT) (c–d). The value that must be added to the heights on the vertical axis to obtain the correct height is shown above the ionograms of oblique sounding (a, c)

was detected at 15:16 LT (19:16 UT) while the ship was moving away from *Vernadsky*. The ionograms of vertical and oblique sounding were recorded during synchronous variations in spectrograms of the *Vernadsky* signal received at the RV *Noosfera* and PL610 (Fig. 4, 5, 12 c, d). These ionograms allow us to determine the mode composition of the signal at the RV.

It is essential for interpreting the dynamics of Doppler frequency shift variations. Three spatial

modes can be detected in the ionogram at 13:46 LT (17:46 UT, Fig. 12 c, ionogram traces are marked in red), and the maximum usable frequencies of two of them are higher than the frequency of the probe signal transmitted from *Vernadsky* (25277 kHz). Clearly, this is the reason why we see two spectral components during the negative Doppler frequency shift variation at 17:36–17:46 UT at the sudden start of a geomagnetic storm (Fig. 4).

3 Results and discussion

Comprehensive ionospheric HF soundings on many radio paths and with various means during the beginning of a powerful geomagnetic storm, which became the strongest in terms of planetary indices over the past five years, allow us to distinguish many features of HF signal propagation on different, including long-distance, radio paths. This became possible due to increased ionospheric plasma velocities relative to the quiet days during the geomagnetic storm. As a result, the magnitudes of Doppler frequency shift variations of ionospheric signals are raised, which, in turn, simplifies the separation of their spectral and spatial modes in the data.

Variations in the spectra of the signals emitted from *Vernadsky* and received at the RV *Noosfera* and the PL610 station are very similar in morphology that was observed during one of the types of self-scattering (Zalizovski et al., 2009; Yampolski et al., 2019). The signals received at spatially very distant points, RV and PL610 (Fig. 3), demonstrate an unexpectedly high level of correlation (Fig. 4, 5).

We should also note that the same high level of correlation of the Doppler frequency shift variations is observed with the variations of the X component of the geomagnetic field at the AIA geomagnetic observatory, which is located at *Vernadsky*, at the same site as the transmitter, and anticorrelation with the Y component at the BEL observatory (Poland) located not far from the receiver. Figures 4 and 5 demonstrate the geomagnetic field variations shown on spectrograms. As can be seen, the variations are similar to each other during the initial stage of the storm. After 19:30 UT, when magnitudes of geomagnetic field variations grew significantly, the signal spectra became much wider and disappeared later.

It should also be noted that a comparison of the dynamics of HF signals with variations of the geomagnetic field at the Ascension Island observatory (not presented here to conserve space) shows the absence of a significant correlation be-

tween them. The mere presence of such a correlation suggests that Doppler frequency shift variations are associated with plasma drifts near the transmitting and/or receiving points. So, we note that the parameters of the signals are correlated with the geomagnetic field variations near the transmitter and receiver.

During the negative deviation of the Doppler frequency shift of the 25277 kHz signal around 17:40 UT, the spectral analysis allows us to detect at least two spectral components both at the RV *Noosfera* and PL610. The only difference between receiving sites is various relative amplitudes of Doppler frequency shift variations for different spectral components, which we will use to explain the observed effects.

Let us start with the signal recorded at the RV *Noosfera* (Fig. 4). The reasonable assumption is that we are dealing with the first two spatial modes propagating due to one-, and two-hop reflections from the ionosphere. This can be confirmed by the oblique ionogram at 13:46 LT (17:46 UT, Fig. 12 c, the ionogram traces are marked in red). As can be seen, two spatial modes propagate between *Vernadsky* and RV *Noosfera* at a frequency of 25277 kHz. Actually, two spectral modes are detected at this time in the spectrogram of the signal propagating on the *Vernadsky* – RV *Noosfera* paths (Fig. 4).

Let us estimate the vertical velocity of the ionospheric layer based on the data of the two spectral modes of the remote sensing signal. In the approximation of equivalent triangles (Davies, 1990), we can estimate the reflection height, signal departure, and arrival angles for the spherically-stratified ionosphere (note that this approximation is far beyond the scope of application for the first spatial mode propagating by one hop to a distance of 4700 km). The results of calculations of the parameters of signal propagation and ionospheric plasma motion based on the data of Doppler sounding of the ionosphere on the *Vernadsky* – RV *Noosfera* path at a frequency of 25277 kHz, as well as oblique sounding based on the signals of the active ionosonde at *Vernadsky* and the

passive one on board the RV *Noosfera* at 17:37–17:40 UT on April 23, 2023 are shown in Table 2. The estimates of the vertical velocity coincide quite well for the first two spatial modes. Typically, for the first mode (one-hop reflection), the estimate of layer upward velocity is 5–6 m s⁻¹ higher than for the second mode (two-hop reflections from the ionosphere).

To explain the spectral composition of the signal at the PL610 station (Fig. 5), we assume that the signal propagates by the same mode, which is received at the RV *Noosfera* as the first one. The length of the first hop is equal to the distance between *Vernadsky* and RV *Noosfera*, which is 4680 km. The distance from *Vernadsky* to the PL610 station is 14770 km. The ratio between the two distances is 3.16. However, since the elevation of the first mode at a distance of 4680 km is 0 degrees, it is impossible to round the minimum number of hops on the *Vernadsky*–PL610 path downward because the elevation of the signal ray becomes negative. We will assume that the first mode propagating from *Vernadsky* to the PL610 station is a four-hop mode, i.e., the signal is reflected four times from the ionosphere. We can assume that the second spectral mode, visible in the signal spectrum, propagates as a five-hop mode. The calculations will be performed for a virtual reflection height of 425 km. The esti-

mates of the average vertical velocity for the two spatial modes are given in Table 3. Table 3 contains the results of calculations of the parameters of signal propagation and ionospheric plasma motion based on Doppler sounding of the ionosphere on the *Vernadsky*–PL610 path at a frequency of 25277 kHz, as well as oblique sounding based on signals from the active ionosonde at *Vernadsky* and the passive ionosonde at RV *Noosfera* at 17:37–17:40 UT on April 23, 2023.

As shown in Table 3, the average values of the vertical velocity of the reflecting layer on the long-distance radio path are significantly lower than the estimates on the shorter *Vernadsky*–RV *Noosfera* path. In order to reconcile the results on the two traces, it can be assumed that the contribution to the Doppler frequency shift occurs only at a limited number of hops. A consistent solution for the two paths can be obtained if we assume that only two reflections cause the Doppler frequency shift on the long-distance radio path. In this case, the estimates of the vertical velocity of the reflecting layer for both radio paths become closer to each other, within 38–46 m s⁻¹ upward.

Let us now turn to the signals of the time signal radio stations. The improvement of the propagation conditions of the CHU station signals at 7850 and 14670 kHz in the first hours of the storm (19–20 UT) both in the meridional direction to

Table 2. The results of calculations of the parameters of signal propagation and ionospheric plasma motion based on the data of Doppler sounding of the ionosphere on the *Vernadsky*–RV *Noosfera* path

Time, UT	Spectral (spatial) mode number	Half the length of the group path, km	Doppler frequency shift, Hz	Average vertical layer velocity, m s ⁻¹	Equivalent height of signal reflection, km	Elevation of the signal output, degrees
17:37:23	2	2550	-5.5	-40	415	14
17:37:23	1	2450	-2.8	-46	454	0
17:38:23	2	2550	-6.4	-46	415	14
17:38:23	1	2450	-3.2	-53	454	0
17:38:54	2	2550	-6.4	-46	415	14
17:38:54	1	2450	-3.1	-51	454	0
17:39:33	2	2550	-6.2	-45	415	14
17:39:33	1	2450	-3.1	-51	454	0

Vernadsky (Fig. 7) and in the direction inclined relative to the meridian to RV *Noosfera* (Fig. 9) looks quite unexpected. It should be noted that it is afternoon over the transmitter, and all receivers are near the solar terminator (Fig. 3).

The spectrum of the signal observed at a frequency of 7850 kHz at all receiving sites is quite wide, of the order of 10 Hz or more. It is not clear at all how absorption can decrease during the start of a geomagnetic storm and create the conditions for long-distance HF propagation along direct illuminated paths. In other words, the appearance of the CHU station signal propagation at 19–20 UT along direct paths seems impossible. However, it can be reasonably assumed that the wide spectra of the signals indicate that they propagated and scattered on the inhomogeneities of the strongly disturbed ionospheric plasma. Intense ionospheric disturbances are characteristic of the auroral ionosphere, especially during magnetic storms. At the initial stage of the storm under consideration, conditions for signal propagation towards the polar ovals may appear due to the rapid upward rise of the ionosphere that we have detected (see height-time-diagrams in Figure 11 a, c, at 15–16 LT that corresponds to 19–20 UT). These signals are scattered on the plasma inhomogeneities of the oval and propagate along trajectories lying far from the sub-solar point, along which the absorption is lo-

wer than along the direct paths. Thus, it can be assumed that the CHU station signal at 19–20 UT propagated to *Vernadsky* and possibly to the RV *Noosfera* via reverse paths. Unfortunately, we do not have pulse selection for the CHU station signals, so it is impossible to confirm this hypothesis.

The RWM station signals of 9996 and 14996 kHz propagated at the beginning of the magnetic storm both to the RV *Noosfera* and *Vernadsky* along direct paths or along lateral trajectories that are no more than 1500 km longer than direct ones (Fig. 10). The gradual increase in the propagation time of the signals with the increase of the Doppler frequency shift module indicates their focusing on regular horizontal gradients of electron concentration, most likely the solar terminator, which is gradually moving away to the west (Fig. 3). However, the same effects were observed at the RV *Noosfera* and *Vernadsky* both before and after the storm day, so they are not storm effects.

It is worth noting that the last oblique ionogram at the RV *Noosfera* was recorded after the beginning of the storm under consideration, namely at 15:16 LT (19:16 UT) at a distance of 4700 km between the active (Fig. 12b) and passive ionosondes (Fig. 12 a). At the same time, a short-term appearance of the CHU station signals at 7850 and 14670 kHz high above the atmospheric noises at *Vernadsky* (Fig. 7), RV *Noosfera* (Fig. 9), and the PL610 station

Table 3. The results of calculations of the parameters of signal propagation and ionospheric plasma motion based on Doppler sounding of the ionosphere on the *Vernadsky*–PL610 path

Time, UT	Spectral (spatial) mode number	Length of one hop, km	Doppler frequency shift, Hz	Average vertical layer velocity, m s ⁻¹	Equivalent height of signal reflection, km	Elevation of the signal output, degrees
17:37:23	5	2954	–5.95	–19	425	9
17:37:23	4	3693	–4.7	–20	425	4
17:38:23	5	2954	–6.9	–22	425	9
17:38:23	4	3693	–5.38	–23	425	4
17:38:54	5	2954	–6.36	–20	425	9
17:38:54	4	3693	–5.0	–21	425	4
17:39:33	5	2954	–6.3	–20	425	9
17:39:33	4	3693	–4.75	–20	425	4

were observed. This coincidence may mean that the propagation conditions of HF signals became better globally at the beginning of the storm (i.e., at different frequencies and radio links). This may be the effect of the storm, during which the movement and redistribution of the ionospheric plasma in space lead to the formation of HF propagation channels that are not present under calm ionospheric conditions.

4 Conclusions

At the beginning of 2022, a radiophysical observatory was deployed on board the RV *Noosfera*, which aims to measure the state of geospace, thunderstorm activity, and characteristics of the waved sea surface. The vessel's observatory has been operating during two voyages of the RV *Noosfera* to Antarctica. The first one (not described in this study) was in January–April 2022 (Odesa – Punta Arenas – *Vernadsky* – Punta Arenas). The second one (discussed in this paper and presented on Figure 1), in March–April 2023 during the navigation along the route Punta Arenas – *Vernadsky* and *Vernadsky* – Arctowski Polish Antarctic Station – Cape Town. During both campaigns, measurements of the characteristics of the HF radio signal propagation were performed.

Multi-position comprehensive measurements using far-spaced transmitting and receiving positions (one of them is on board a moving vessel) were performed to suggest mechanisms of HF propagation over various, including long-distances, paths, as well as to solve the inverse problem of restoring the parameters of ionospheric plasma motion. The measuring campaign was supported by the vertical sounding of the ionosphere at *Vernadsky* and oblique ionospheric sounding by the signals emitted from *Vernadsky* and registered by a passive ionosonde on board the RV *Noosfera*.

The April 23, 2023, geomagnetic storm was used as a case study. The beginning of the storm brought the ionospheric plasma into intense motion, which manifested in Doppler frequency shifts of HF signals on different radio paths. That, in turn, was used to

select the spectral and corresponding spatial modes of signal propagation. According to observations and data analysis, we obtained the following results.

The HF signals emitted from *Vernadsky* and recorded at the RV *Noosfera* and the PL610 station during the first hours of the geomagnetic storm demonstrate a high correlation of variations in their spectral characteristics. In turn, the variations of the Doppler frequency shift of the signals at both locations correlate well with the variations of the Earth's magnetic field components measured by the AIA geomagnetic observatory operating at *Vernadsky* and the BEL geomagnetic observatory. This indicates that the plasma motions measured in variations of Doppler frequency shift were caused by the drift.

Relatively large Doppler frequency shifts of the signals during the sudden commencement of the geomagnetic storm made it possible to separate several spatial modes. Using that effect, it was shown that the signal on the *Vernadsky*–RV *Noosfera* radio path propagated by one- and two-hop spatial modes. Supplementing the Doppler measurements with oblique ionospheric sounding with a receiving position on board the RV *Noosfera* allowed solving the problem of propagation on the *Vernadsky*–RV *Noosfera* path more rigorously, measure the parameters of two signal's spatial modes and estimate the vertical velocity of the plasma layer in the first minutes of the storm at 40–53 m s⁻¹ upward.

Using the information on the mode composition of the HF signal propagating to the RV *Noosfera*, it is reasonable to assume that the signal propagated to the PL610 station by four- and five-hop spatial modes. The average velocity of the plasma layer at the reflection points was estimated from the signals recorded at the PL610 station. The estimate was half as high as the average velocity on the *Vernadsky*–RV *Noosfera* path. However, assuming that the Doppler frequency shift is caused by the plasma motion at two reflection points only, for example, the first and the last, the solution of the problem is consistent with that obtained for the *Vernadsky*–RV *Noosfera* path, the

estimated vertical velocity of the plasma layer is approximately $38\text{--}46\text{ m s}^{-1}$ upward.

After the beginning of the geomagnetic storm, the last occurrence of an oblique trace on the ionogram was registered when the RV *Noosfera* was approximately 4700 km away from the active ionosonde. Concurrently, the CHU station signals at 7850 and 14670 kHz were observed at all receiving sites during a short period of time. This simultaneity possibly suggests that the conditions for HF signal propagation improved globally during the initial hours of the geomagnetic storm. The motion and redistribution of the ionospheric plasma in space led to the formation of HF radio propagation channels that are absent under quiet conditions.

Author contributions. The idea, conceptualization: A.Z., Yu.Y. Conducting experiments: A.Z., O.Bu., O.Bo., B.G., A.S., A.R., V.L. Data acquisition and preparation: O.Bu., O.Bo., A.S., A.R., A.K. Data processing and illustration preparation: A.Z., O.Bo., A.S., A.R., V.L. Methodology: A.Z., Yu.Y., O.K., A.K., S.K. Interpretation of the results: A.Z., I.S., Yu.Y., A.K., S.K. Writing, reviewing and editing: A.Z., Yu.Y., I.S., O.K., O.Bo., A.K. All authors have read and agree to publish the current version of the manuscript.

Acknowledgments. This paper was partially supported by Partner Project P775 (EOARD 22IOE019) between the European Office of Aerospace Research and Development, the Ukrainian Science and Technology Center, and Institute of Radio Astronomy, National Academy of Sciences of Ukraine, and within the program of long-term program of support for Ukrainian research teams at the Polish Academy of Sciences, carried out in cooperation with external partners (agreement number PAN.BFB.S.BWZ.364.022.2023). The work was supported also by Projects “Heliomax-2023” (No 0123U103736) between the National Antarctic Scientific Center and the Institute of Radio Astronomy, and in frames of the budget projects of National Academy of Sciences of Ukraine «Yatagan-4» (No 0121U108635), «Zond-6» (No 0122U000549), and «Prostir-2» (No 0123U102424).

Authors are grateful to Dr. Evgeny Mishin (US Air Force Research Laboratory) for the longterm support and useful discussions of the results, and Dr. Mariusz Pożoga and Łukasz Tomasik (Space Research Centre of Polish Academy of Sciences) for assistance with setting-up the measuring site at the LOFAR PL610 observatory in Borowiec.

Conflict of Interest. The authors declare no conflict of interest.

References

- Broom, S. M. (1984). A new ionosonde for Argentine Islands ionospheric observatory, Faraday Station. *British Antarctic Survey Bulletin*, 62, 1–6.
- Davies, K. (1990). *Ionospheric Radio*. Peter Peregrinus Ltd.
- Galushko, V. G., Koloskov, A. V., Paznukhov, V. V., Reinisch, B. W., Sales, G. S., Yampolski, Y. M., & Zalizovski, A. V. (2008). Self-scattering of HF heater emission observed at geographically dispersed receiving sites. *IEEE Antennas and Propagation Magazine*, 50(6), 155–161. <https://doi.org/10.1109/MAP.2008.4768950>
- Gurevich, A. V., & Tsedilina, E. E. (2011). *Long Distance Propagation of HF Radio Waves*. Springer Berlin Heidelberg.
- Kashcheyev, A. S., Kashcheyev, S. B., Koloskov, A. V., Pikulik, I. I., Bryukhovetski, A. S., & Yampolski, Yu. M. (2003). Bistatic HF Scattering from the Sea Surface. II. Experiment. *Radio Physics and Radio Astronomy*, 8(3), 242–252.
- Kashcheev, S. B., Yampolski, Yu. M., & Zalizovski, A. V. (2001). Bistatic sounding of the sea surface by signals from HF broadcasting stations. *Radio Physics and Radio Astronomy*, 6(1), 79–89.
- Kashcheev, S. B., Zalizovski, A. V., Sopin, A. O., & Pikulik, I. I. (2013). On the possibility of bistatic HF ionospheric sounding by exact time signals. *Radio Physics and Radio Astronomy*, 18(1), 34–42.
- Koloskov, O., Kashcheyev, A., Bogomaz, O., Sopin, A., Gavrylyuk, B., & Zalizovski, A. (2023). Performance analysis of a portable low-cost SDR-based ionosonde. *Atmosphere*, 14(1), 159. <https://doi.org/10.3390/atmos14010159>.
- Koloskov, A. V., Yampolski, Y. M., Zalizovski, A. V., Galushko, V. G., Kascheev, A. S., La Hoz, C., Brekke, A., Beley, V. S., & Rietveld, M. T. (2014). Network of INTERNET-controlled HF receivers for ionospheric research. *Radio Physics and Radio Astronomy*, 19(4), 324–335 <https://doi.org/10.15407/rpra19.04.324> (In Russian)
- Muldrew, D. B., & Maliphant, R. G. (1962). Long-distance one-hop ionospheric radio-wave propagation. *Journal of Geophysical Research. Atmospheres*, 67(5), 1805–1815. <https://doi.org/10.1029/JZ067i005p01805>

- Litvinenko, L. N., & Yampolsky, Yu. M. (Eds.). (2005). *Elektromagnitnyye proyavleniya geofizicheskikh efektov v Antarktide [Electromagnetic manifestation of geophysical effects in Antarctica]*. Institute of Radio Astronomy of National Academy of Sciences of Ukraine. (In Russian)
- Ludwig, G. H. (2011). *Opening space research: Dreams, technology, and scientific discovery*. American Geophysical Union.
- Shlionsky, A. G. (1979). *Dal'neye rasprostraneniye radiovoln v ionosfere [Long-Range Propagation of Radio Waves in the Ionosphere]*. Nauka. (In Russian)
- Stein, S. (1958). The role of ionospheric-layer tilts in long-range high-frequency radio propagation. *Journal of Geophysical Research*, 63(1), 217–241. <https://doi.org/10.1029/JZ063i001p00217>
- Yampolski, Yu., Milikh, G., Zalizovski, A., Koloskov, A., Reznichenko, A., Noss, E., Bernhardt, P. A., Briczinski, S., Grach, S. M., Shindin, A., & Sergeev, E. (2019). Ionospheric non-linear effects observed during very-long-distance HF propagation. *Frontiers in Astronomy and Space Sciences*, 6, 12. <https://doi.org/10.3389/fspas.2019.00012>
- Zalizovski, A. V., Kashcheyev, A. S., Kashcheyev, S. B., Koloskov, A. V., Lisachenko, V. N., Paznukhov, V. V., Pikulik, I. I., Sopin, A. A., & Yampolski, Yu. M. (2018). A prototype of a portable coherent ionosonde. *Space science and technology*, 24(3), 10–22. <https://doi.org/10.15407/knit2018.03.010>
- Zalizovski, A. V., Kashcheyev, S. B., Yampolski, Yu. M., Galushko, V. G., Beley, V., Isham, B., Rietveld, M. T., La Hoz, C., Brekke, A., Blagoveshchenskaya, N. F., & Kornienko, V. A. (2009). Self-scattering of a powerful HF radio wave on stimulated ionospheric turbulence. *Radio Science*, 44(3). <https://doi.org/10.1029/2008RS004111>
- Zalizovski, A., Koloskov, O., Kashcheyev, A., Kashcheyev, S., Yampolski, Y., Charkina, O. (2020). Doppler vertical sounding of the ionosphere at the Akademik Vernadsky station. *Ukrainian Antarctic Journal*, 1, 56–68. <https://doi.org/10.33275/1727-7485.1.2020.379>
- Zalizovski, A. V., Koloskov, A. V., & Yampolski, Yu. M. (2015). Studying in Antarctica the time-frequency characteristics of HF signals at the long radio paths. *Ukrainian Antarctic Journal*, 14, 124–137. <https://doi.org/10.33275/1727-7485.14.2015.181> (In Russian)
- Zalizovski, A., Stanislawska, I., Lisachenko, V., & Charkina, O. (2021). Variability of Weddell Sea ionospheric anomaly as deduced from observations at the Akademik Vernadsky station. *Ukrainian Antarctic Journal*, 1, 47–55. <https://doi.org/10.33275/1727-7485.1.2021.666zaliz>
- Zalizovski, A., Yampolski, Yu., Koloskov, O., Kashcheyev, S., Lisachenko, V., Shvets, A., Kashcheyev, A., & Bogomaz, O. (2022). First results of RF measurements on board the Ukrainian research vessel *Noosfera* on the way to Antarctic Peninsula. *10th SCAR Open Science Conference, 1–10 August 2022, India* (No 845).
- Zalizovskii, A. V., Galushko, V. G., Kashcheev, A. S., Koloskov, A. V., Yampolski, Yu. M., Egorov, I. B., & Popov, A. V. (2007). Doppler selection of HF radiosignals on long paths. *Geomagnetism and Aeronomy*, 47, 636–646. <https://doi.org/10.1134/S001679320705012X>

Received: 22 September 2023

Accepted: 12 January 2024

А. Залізовський^{1, 2, 3, *}, Ю. Ямпольський², І. Станіславська³,
О. Колосков^{1, 2, 4}, О. Буданов², О. Богомаз⁵, Б. Гаврилюк^{1, 2}, А. Сопін^{1, 2},
А. Резниченко^{2, 3}, А. Кашчєєв⁴, С. Кашчєєв², В. Лисаченко²

¹ Державна установа Національний антарктичний науковий центр
Міністерства освіти та науки України, м. Київ, 01601, Україна

² Радіоастрономічний інститут Національної академії наук України, м. Харків, 61002, Україна

³ Центр космічних досліджень Польської академії наук, м. Варшава, 00-716, Польща

⁴ Відділення фізики, Університет Нью-Брансвік, м. Фредеріктон, NB E3B5A3, Канада

⁵ Інститут іоносфери Національної академії наук України та Міністерства
освіти і науки України, м. Харків, 61001, Україна

* Автор для кореспонденції: zaliz@rian.kharkov.ua

**Надалеке поширення ВЧ радіохвиль під час геомагнітної бурі у квітні 2023 року
за результатами вимірювань в Антарктиці, Європі та на борту НДС «Ноосфера»**

Реферат. Метою роботи є експериментальне вивчення механізмів наддалекого поширення високочастотних (ВЧ) радіосигналів, а також просторово-часових варіацій іоносферних параметрів у перші години потужної геомагнітної бурі, що розпочалася 23 квітня 2023 р., за допомогою просторово рознесених вимірювальних засобів,

розташованих на науково-дослідному судні (НДС) «Ноосфера», Українській антарктичній станції «Академік Вернадський» (далі станція «Академік Вернадський») та обсерваторії PL610 мережі LOFAR у Боровці (Польща). У цьому дослідженні використовували методи високочастотного вертикального та похилого зондування іоносфери. На борту НДС розгорнуто радіофізичну обсерваторію. Обсерваторія обладнана приймальною позицією іонозонда та двоканальним доплерівським ВЧ приймачем. Геокосмічні вимірювання проводились синхронно на НДС, станції «Академік Вернадський» та PL610. У перші години геомагнітної бурі 23–24 квітня 2023 року спостерігалися несподівано добре скорельовані варіації доплерівських зсувів частоти ВЧ сигналів, що випромінювались зі станції «Академік Вернадський», на НДС і PL610. Ці ж зсуви частоти добре корелюють з варіаціями магнітного поля, виміряними в Антарктиді і Польщі. Варіації частоти спектральних компонент ВЧ сигналів, виділені завдяки збуреним умовам, використовуються для з'ясування механізму поширення ВЧ сигналів на великі відстані та оцінки вертикальної швидкості іоносферного шару. Несподівана поява сигналів станції CHU на частотах 7850 і 14670 кГц спостерігалася на всіх приймальних пунктах. Найімовірніше, ці радіосигнали, несподівано зареєстровані під час початкової стадії геомагнітної бурі, поширювалися шляхом розсіювання на іоносферних неоднорідностях полярних овалів, і далі зворотними (вздовж довшої дуги великого кола) трасами. Перерозподіл іоносферної плазми під час геомагнітної бурі призводить до формування ВЧ каналів наддалекого поширення радіохвиль, які відсутні за спокійних умов.

Ключові слова: геомагнітне поле, доплерівський ВЧ приймач, іонозонд, іоносфера